HHS Public Access

Author manuscript

J Invest Dermatol. Author manuscript; available in PMC 2024 October 01.

Published in final edited form as:

J Invest Dermatol. 2023 October ; 143(10): 1964–1972.e4. doi:10.1016/j.jid.2023.03.1662.

Ligand-activation of the aryl hydrocarbon receptor up-regulates epidermal UDP-glucose ceramide glucosyltransferase and glucosylceramides

Carrie Hayes Sutter[1], **Shafquat Azim**[1,*], **Anyou Wang**[1], **Jyoti Bhuju**[1,*], **Amelia S. Simpson**[1], **Aayushi Uberoi**[3], **Elizabeth A. Grice**[3], **Thomas R. Sutter**[1,2]

[1]Department of Biological Sciences, University of Memphis, Memphis, TN 38152, USA

[2]Department of Chemistry, University of Memphis, Memphis, TN 38152, USA

[3]Department of Dermatology, Perelman School of Medicine, University of Pennsylvania, Philadelphia, PA 19104, USA

Abstract

Ligand-activation of the aryl hydrocarbon receptor (AHR) accelerates keratinocyte differentiation and the formation of the epidermal permeability barrier (EPB). Several classes of lipids, including ceramides, are critical to the EPB. In normal human epidermal keratinocytes, the AHR ligand, 2,3,7,8-tetrachlorodibenzo-*p*-dioxin (TCDD), increased RNA levels of ceramide metabolism and transport genes, UDP-glucose ceramide glucotransferase (UGCG), ATP binding cassette subfamily A member 12 (ABCA12), glucosylceramidase beta (GBA1) and sphingomyelin phosphodiesterase 1 (SMPD1). Levels of abundant skin ceramides were also increased by TCDD. These included the metabolites synthesized by UGCG, glucosylceramides and acyl glucosylceramides. Chromatin immunoprecipitation-sequence analysis and luciferase reporter assays identified UGCG as a direct AHR target. The AHR antagonist, GNF351, inhibited the TCDD-mediated RNA and transcriptional increases. Tapinarof, an AHR ligand approved for the treatment of psoriasis, increased UGCG RNA, protein and its lipid metabolites hexosylceramides, as well as increased the expression of ABCA12, GBA1 and SMPD1. In *Ahr*-null mice, *Ugcg* RNA and hexosylceramides were lower compared to wild-type. These results indicate that the AHR regulates the expression of UGCG, a ceramide metabolizing enzyme required for ceramide trafficking, keratinocyte differentiation, and EPB formation.

Correspondence: Thomas R. Sutter, Department of Biological Sciences, 239 Ellington Hall, 3700 Walker Avenue, University of Memphis, Memphis, TN 38152, USA. tsutter@memphis.edu.

*Affiliation of authors at the time the work was performed. Current author affiliations are provided in Supplementary Materials online.

AUTHOR CONTRIBUTIONS

Conceptualization: CHS, EAG, TRS; Data Curation: CHS, AW; Formal Analysis: CHS, SA, AW, ASS; Funding Acquisition: EAG, TRS; Investigation: CHS, SA, AW, JB, ASS, AU, EAG, TRS; Methodology: CHS, SA, AW, TRS; Project Administration: CHS, EAG, TRS; Resources: EAG, TRS; Supervision: CHS, EAG, TRS; Validation: CHS, SA, ASS; Visualization: CHS, AW, TRS; Writing – Original Draft Preparation: CHS, AW, TRS; Writing – Review and Editing: CHS, SA, AW, JB, ASS, AU, EAG, TRS

CONFLICT OF INTEREST The authors declare no conflict of interest.

INTRODUCTION

One of the most important functions of the skin is to form the epidermal permeability barrier (EPB) to prevent water loss and inhibit exposures to pathogens, chemicals, and ultraviolet irradiation. The EPB consists of the stratum corneum (SC), the outer most layers of the skin, and tight junctions, the intercellular barriers below the SC. The SC is made up of corneocytes and a lipid extracellular matrix consisting primarily of cholesterol, free fatty acids and ceramides. Keratinocytes in the stratum granulosum (SG) secrete lipids that form organized and dynamic bilayer sheets. Within these layers the acylceramides (ultra-long chain ω-O-acylceramides) covalently crosslink to the cornified envelope proteins to provide a scaffold for lipid matrix assembly (Norlen et al., 2022).

Ceramides constitute nearly 50 percent of the epidermal lipid matrix mass of the SC. Each ceramide is composed of a fatty acid linked by an amide bond to a sphingoid base, the combinations of which determine their specific subclasses (Table S1) (Fujii, 2021, Rabionet et al., 2014). Following *de novo* synthesis in the endoplasmic reticulum (ER), the trafficking of ceramides is complex and distinct for the specific ceramide subclasses derived from sphingomyelin (SM) and various glycosphingolipids (GSL) (Yamaji and Hanada, 2015). The most abundant epidermal GSLs are glucosylceramides (GlcCers) (Hamanaka et al., 2002). GlcCers, which includes acylGlcCers, are synthesized by the addition of glucose to the hydroxyl head group of ceramides by the membrane bound UDP-glucose ceramide glucotransferase (UGCG), located at the cytosolic surface of the cis/medial Golgi cisternae (Chujor et al., 1998). Movement of GlcCers into the lamellar bodies is facilitated by ATP binding cassette subfamily A member 12 (ABCA12). At the interface between the SG and SC, GlcCers are secreted extracellularly from the lamellar bodies where glucosylceramidase beta (GBA1) catalyzes the removal of glucose to regenerate the hydrophobic ceramides, facilitating their dehydration, unfolding and assembly into lipid lamellae (Boer et al., 2020b, Fujii, 2021, Norlen et al., 2022) (Figure 1a).

Ligand activation of the aryl hydrocarbon receptor (AHR), a transcription factor that heterodimerizes with the aryl hydrocarbon receptor nuclear transporter (ARNT), promotes keratinocyte differentiation in part by regulation of metabolic reprogramming and elevating expression of genes and pathways important to keratinocyte differentiation and the formation of the EPB (Kennedy et al., 2013, Sutter et al., 2011, Sutter et al., 2019, Tsuji et al., 2017). In human keratinocytes activation of the AHR with 2,3,7,8-tetrachlorodibenzo-*p*-dioxin (TCDD), a potent and selective ligand, increases the RNA expression of numerous enzymes of the sphingolipid pathway, along with their lipid products (Kennedy et al., 2013, Sutter et al., 2009). In mice, *in utero* exposure to TCDD similarly increases epidermal ceramide levels and accelerates the development of the EPB by one day (Bhuju et al., 2021, Muenyi et al., 2014, Sutter et al., 2011). Knock-out of the AHR as well as an AHR-ligand restrictive diet impair barrier repair in mice. Conversely, dietary exposure to an AHR ligand improves barrier repair (Haas et al., 2016). Activation of murine skin AHR by colonization with commensal bacteria is critical to the proper formation and function of the EPB and contributes to barrier recovery following injury (Uberoi et al., 2021). A clinically approved bacterially derived AHR ligand, tapinarof, has had recent success in treating psoriasis in adults (Lebwohl et al., 2021). These outcomes are likely due to its anti-inflammatory and

pro-differentiation characteristics (Smith et al., 2017). The effect of tapinarof on ceramide metabolism has yet to be reported.

Here, we studied genes and products of ceramide metabolism and report on the transcriptional regulation of UGCG by activation of the AHR by TCDD. Additionally, we compared TCDD and tapinarof responses in human keratinocytes by measuring gene expression and GSL production. Lastly, studies in the skin of *Ahr* knock-out mice investigated a physiological role of the AHR in maintaining epidermal UGCG expression and its GSL products, hexosylceramide (HexCers).

RESULTS

Ligand activation of the AHR is associated with altered expression of Cer metabolic and transport genes and increased levels of glucosylated Cer precursors, GlcCer and acylGlcCer.

The effects of activation of the AHR on the enzymes and transporters involved in the post-ER production of the abundant SC ceramides were measured in NHEKs. Treatment of NHEKs with the potent and selective AHR ligand TCDD (10 nM) for 24 h increased the RNA expression of UGCG, ABCA12, GBA1, and SMPD1, and decreased the expression of B4GALT5. These changes were inhibited by cotreatment with the AHR antagonist, GNF351 (100 nM), indicating that ligand activation of the AHR was required for these effects of TCDD. Expression of CERT1, SGMS1 and SGMS2 RNAs were not significantly changed by treatment (Figure 1b).

Consistent with the elevation of UGCG, relative levels of the glucosylceramides, GlcCer1 (1.24-fold), GlcCer2 (1.20-fold) and acylGlcCer (1.41-fold) were increased by treatment of NHEKs with TCDD for 72 h. Similar increases were observed in several non-glucosylated ceramide subclasses including NP (1.45-fold), NH (1.75-fold), AP (1.72-fold), AH (1.69-fold), and AS (1.52-fold). The level of NS was unchanged, and the acylCers, EOS, EOP, and EOH were not detected by this high-performance thin layer chromatography (HPTLC) analysis (Figure 1c). While the glucosylated ceramides reflect post-ER metabolism, levels of the non-glucosylated ceramides may reflect *de novo* synthesis in the ER as well as post-ER metabolism.

Chromatin immunoprecipitation-sequencing (ChIP-Seq) identified AHR binding near the transcriptional start site (TSS) of UGCG

To interrogate ligand-activated AHR-genome interactions we carried out ChIP-Seq experiments in NHEKs exposed to TCDD. Of the possible ceramide metabolism targets identified in Figure 1b, UGCG, SMPD1 and B4GALT5 had AHR binding sites within 5 kb of their TSSs. While each of these genes is important to ceramide metabolism, we focused on the regulation of UGCG because of its importance in the metabolism and trafficking of most of the SC ceramides (Amen et al., 2013, Jennemann et al., 2007).

Exposure of NHEKs to TCDD (10 nM) for 45 min increased the binding of the AHR at the genomic location 111896536–111896739 on chromosome 9. This site ends 26 base pairs upstream of the UGCG TSS (Figure 2a). To determine whether binding of the AHR at this

site also affected transcription, this region was cloned into a luciferase reporter vector and transfected into NHEKs. Exposure to TCDD increased the reporter activity compared to the vehicle control (Figure 2b–c, e). Furthermore, this increase was blocked by the addition of the AHR antagonist, GNF351 (100 nM), demonstrating the role of ligand activation of the AHR in this effect (Figure 2c). To provide additional evidence for a role of the AHR in activating transcription of UGCG from this region, specific mutations were made in the sites most closely matching the AHR:ARNT binding site consensus, 5'-GCGTG-3', identified in this target sequence (Figure 2d). Mutations were made in the two highest ranking consensus sites. Site 1 scored 0.92 and site 2 scored 0.81 (Figure 2d). Mutation of the lower-ranked AHR consensus site 2 (MT2) did not affect reporter activity. But mutation of the higher-ranked consensus site 1 (MT1) decreased the reporter activity of both the vehicle- and TCDD-treated samples compared to the WT reporter construct (Figure 2e), indicating that the AHR binds to this consensus site and activates transcription from this site.

Increased expression of UGCG and HexCers in response to the therapeutic AHR ligand, tapinarof

The AHR ligands, TCDD (10 nM) and tapinarof (3 μM), affected RNA expression of Cer-related genes similarly. Treatment of NHEKs for 24 h with either ligand increased the expression of UGCG, ABCA12, GBA1 and SMPD1 RNA, each approximately 2-fold, while levels of B4GALT5 RNA were decreased about 2-fold (Figure 3a). Following 48 h of treatment, TCDD or tapinarof elevated levels of UGCG protein expression by approximately 8–10-fold (Figure 3b). Following 72 h of treatment, TCDD or tapinarof increased levels of HexCers about 30%, consistent with elevated UGCG protein (Figure 3c). Measurements of HexCers include both GlcCers and GalCers. However, as GalCers are found in a limited number of cells and tissues, and not in skin and keratinocytes (Reza et al., 2021), GlcCer is the predominant metabolite in HexCer measurements. LacCers, the product of B4GALT5, were decreased about 50% by either treatment (Figure 3c). LacCer levels in keratinocytes are quite low compared to other Cer metabolites and their roles in keratinocyte differentiation have not yet been elucidated. These data indicate that the regulation of the RNA by these AHR ligands results in similar changes in enzyme and ceramide metabolite levels.

Murine UGCG and its lipid products, HexCers, are dependent on the *Ahr*

The expression of *Ugcg* RNA and the UGCG-associated epidermal lipid products, HexCers, were significantly decreased in the skin of *Ahr* knock-out mice compared to the skin samples of *Ahr* wild-type mice (Figure 4a). Neither murine *B4galt5* RNA or the lipid products of B4GALT5, LacCers, were significantly affected in the skin of *Ahr* knock-out compared to the *Ahr* wild-type mice (Figure 4b). Although human and murine UGCG both appear to be regulated by the AHR, sequence alignments of human and murine UGCG genomic DNA showed a lack of conservation at the putative response element identified in Figure 2d and e, suggesting that the regulation by the AHR may differ between these two species.

DISCUSSION

The ceramide metabolic process investigated here is often described as the Cer salvage pathway. In the epidermis, the enzymes and transporters involved in salvaging Cers are critical to the formation of the EPB. Disruptions in numerous salvage pathway genes, UGCG, SGMS2, ABCA12, SMPD1, and GBA1, are each linked to skin diseases in humans and/or animal models, most of which are severe (Kelsell et al., 2005, Monies et al., 2018, Nomoto et al., 2018, Schmuth et al., 2000, Sidransky et al., 1992). Genetic studies in mice demonstrate that UGCG is essential to keratinocyte differentiation, wound healing, and the formation and function of the EPB (Amen et al., 2013, Jennemann et al., 2007, Yamashita et al., 1999). In humans, a mutation in UGCG is proposed to be a factor in a rare autosomal recessive form of severe ichthyosis (Monies et al., 2018). Glucosylation of Cers by UGCG is critical to their localization, topology, and trafficking in the Gogli (Yamaji and Hanada, 2015), yet despite this understanding of its function, little is known about its regulation in keratinocytes. Here we report that UGCG is a transcriptional target of the ligand activated AHR in human keratinocytes. This mechanism is consistent with the observed increases in RNA, protein, and products of UGCG, GlcCer and acylGlcCer. The physiological importance of this regulation is supported by our findings that *Ugcg* RNA and HexCer levels in the skin of *Ahr* knock-out mice are reduced compared to the WT mice. These findings are consistent with studies in murine sciatic nerves where *Ugcg* RNA and HexCer levels are also dependent on the *Ahr* (Majumder et al., 2020).

It seems likely that the AHR-mediated increases in Cer production are due to increases in the enzymes and transporters of salvage pathway reported here (UGCG, GBA1, SMPD1 and ABCA12) and to increases in the Cer *de novo* synthesis pathway. In human keratinocytes, activation of the AHR with TCDD increases RNA levels of one of the rate-limiting *de novo* synthesis enzymes of the serine palmitoyltransferase long chain (SPTLC) complex, SPTLC3, as well as the RNA levels of *de novo* synthesis enzymes, delta 4-desaturase, sphingolipid 2 (DEGS2) and ceramide synthase 3 (CERS3) (Kennedy et al., 2013). In mice, activation of the AHR with tetrachlorodibenzofuran transcriptionally increases the RNA expression of *Sptlc2* as well as the RNA levels of several other hepatic *de novo* synthesis enzymes resulting in hepatic ceramide accumulation and lipogenesis (Liu et al., 2021). Another member of the SPTLC complex, the small subunit, *Sptssa*, is also transcriptionally regulated by the AHR and knock-out of the *Ahr* associates with decreased expression of ceramide synthesis genes and ceramide levels in several murine tissues including liver, lung and sciatic nerve (Majumder et al., 2020).

TCDD is the most potent AHR ligand and is the prototype of a large set of environmental pollutants known as dioxin-like chemicals. TCDD is resistant to degradation and bioaccumulates in many organisms including humans. Accidental human exposures to high levels of TCDD or dioxin-like chemicals results in a skin condition termed chloracne, characterized by hyperplasia and hyperkeratosis of the interfollicular epidermis, hyperkeratosis of the hair follicle, involution of the sebaceous glands, and comedone and cyst formation (Saurat et al., 2012). The potential contributions of ceramides to this condition have not been investigated.

While the toxic effects of TCDD, including cancer, preclude its use as a therapeutic compound, studies of this potent and selective AHR ligand showed that AHR activation accelerates keratinocyte differentiation and the formation of the EPB (Kennedy et al., 2013, Sutter et al., 2011, Sutter et al., 2009). Therapeutic indications for AHR ligands in the treatment of skin diseases followed, demonstrating that activation of the AHR constituted a mechanism of action of coal tar in the treatment of AD (van den Bogaard et al., 2013), as well as for the anti-inflammatory effects of 6-formylindolo(3,2b)carbazole in models of psoriasis (Di Meglio et al., 2014). Tapinarof, a bacterial stilbenoid, was identified in a chemical screen as an AHR ligand that resolved skin inflammation in mouse and human models of psoriasis. Tapinarof is approved for the treatment of plaque psoriasis (Lebwohl et al., 2021, Smith et al., 2017) and clinical trials are ongoing for the treatment of AD (Paller et al., 2021). Here we show that in human keratinocytes the increases in UGCG and its HexCer products are similar for tapinarof and TCDD, resembling their similar effects on epidermal barrier gene expression (Kennedy et al., 2013, Smith et al., 2017). As ceramides play a critical role in EPB function and wound healing (Uchida and Park, 2021, van Smeden et al., 2014), and both topical ceramides and oral GlcCer are reported to improve EPB (Uchida and Park, 2021), the understanding of how AHR ligands, especially those with therapeutic potential (Smith et al., 2017, van den Bogaard et al., 2013), affect ceramide metabolism warrants further study.

Imbalances in ceramides are reported in several skin diseases such as AD and psoriasis (Fujii, 2021, Uchida and Park, 2021, van Smeden et al., 2014). While there is an overall reduction of ceramides in AD and psoriasis, most notably in acylCers, NP, and NH, increases in AS and NS ceramides are also consistently observed. Compared to healthy control skin samples, decreased ratios of levels of NP, NH, and AH to AS or NS correlate with worsened skin functionality (Fujii, 2021, van Smeden et al., 2014, Yokose et al., 2020). In addition, an increase in GlcCer is reported in AD (Toncic et al., 2020). To understand these changes several studies have focused on GBA1 and SMPD1 protein expression and/or enzymatic activity due to the importance of these enzymes in stratum corneum ceramide formation. Many, but not all, of the studies report an increase in SMPD1 activity, which correlates with increased AS and NS levels, and a decrease in GBA1, which correlates with the decrease in the other ceramides (Alessandrini et al., 2004, Boer et al., 2020a, Danso et al., 2017, Jensen et al., 2004, Jin et al., 1994, Kusuda et al., 1998). For AD, the localization of these two active enzymes is also reported to change (Danso et al., 2017). It is not well understood how these changes in ceramide synthesizing and metabolizing enzymes occur in AD or psoriasis. Analyses of differential gene expression comparing AD or psoriasis samples to healthy controls fail to identify ceramide metabolic process as a functional class (Hu et al., 2022, Schwingen et al., 2020, Tsoi et al., 2019). Of the members of this category, only SPTLC2 RNA is reported as increased in lesional AD relative to healthy control skin (Hu et al., 2022), suggesting that *de novo* ceramide synthesis may be increased in AD. Additional studies will undoubtedly improve our understanding of the importance and regulation of GBA1, SMPD1, and other ceramide biosynthetic and metabolizing enzymes in the alteration of ceramides in skin diseases such as AD and psoriasis.

In addition to skin disorders, imbalances in ceramides and their metabolites are implicated in cardiovascular, metabolic, infectious, psychological, and neurodegenerative diseases as

well as in asthma and cancer (Bernal-Vega et al., 2023, Diaz-Perales et al., 2021, Green et al., 2021, Gulbins and Li, 2006, Janneh and Ogretmen, 2022, Li and Kim, 2021). Interestingly, most of these diseases are also comorbidities of psoriasis and AD (Menter et al., 2018, Thyssen et al., 2023). While the reasons for this are not well understood, it is noteworthy that exposure of mice to toxic AHR ligands causes non-alcoholic fatty liver disease and steatohepatitis (Fling et al., 2020, Nault et al., 2016), accompanied by increased ceramide synthesis (Liu et al., 2021). Emerging knowledge links ceramides and metabolic disease (Green et al., 2021) and studies report that inhibition of UGCG can enhance insulin sensitivity (Aerts et al., 2007) and block hepatic steatosis in mice (Zhao et al., 2009). Overall, studies are just beginning to uncover the role of the AHR in the regulation of ceramide biosynthesis and metabolism. Such knowledge should improve our understanding of the impact of the AHR in disease causing and health promoting mechanisms related to ceramide metabolism.

MATERIALS AND METHODS

Cell Culture

Neonatal NHEKs from multiple donors, 417, 9047, and 4249 (Lonza, Walkersville, MD), were grown as previously described (Sutter, Yin et al. 2009, Tran, Kennedy et al. 2012). Lonza verifies that these cells are mycoplasm-, bacteria-, yeast- and fungi-free. The use of human keratinocytes was reviewed by the University of Memphis Institutional Review Board. Donor consent was not required by the University of Memphis Institutional Review Board because it was determined that the cells were not collected specifically for this study, and do not have identifiers. Therefore, the use of these cells from this source are presumptively considered to be research not involving human subjects. These cells were considered by the institutional biosafety committee. All works with these cells was performed as prescribed using biosafety level 2 practices. Cells at passage 5 were grown to 95–100% confluence in complete KSFM before pretreatment in basal KSFM for 24 h, followed by treatment in basal KSFM as indicated below.

Chemicals

The following chemicals were purchased from MilliporeSigma (Billerica, MA): DMSO (0.1%, D2650); GNF351 (100 nM, 182707). Tapinarof was purchased from MedChemExpress (3 μM, Monmouth Junction, NJ, HY-109044). The concentration of TCDD used was 10 nM. Induction of the AHR biomarker, CYP1A1 RNA, was used to determine that 3 μM tapinarof was equally effective as 10 nM TCDD.

RNA isolation

For all RNA studies, cells were treated for 24 h. Total RNA isolation was performed as previously described using RNA Stat-60 (Tel-Test, Friendswood, TX) (Sutter, Yin et al. 2009). RNA concentration was determined using a Nanodrop 2000 (ND-2000, ThermoFisher, Waltham, MA).

Quantitative PCR

RNA was reverse transcribed using MMLV (28025021) with RNaseOut (10777019) (ThermoFisher). For quantitation, individual efficiencies for each primer pair were used. Samples were normalized to values of TBP (human) and EEF2 (mouse). Primers and efficiencies used in this study are listed in Supplemental Table 2.

Antibodies

The following primary antibodies were used for immunoblotting: ACTB (A5441, 1:100,000, Sigma Aldrich) and UGCG (ab197369, 1 μg/ml, Abcam). The HRP-linked secondary antibodies were goat anti-rabbit (111035144, 1:10,000, Jackson ImmunoLaboratories Research, West Grove, PA) and goat anti-mouse (115035003, 1:10,000, Jackson ImmunoLaboratories Research). For ChIP-Seq analyses an AHR antibody was used (BMLSA210, Enzo, Farmingdale, NY).

Animals

Ahr knock-out mice, B6.129-Ahrtm1Bra/J (Schmidt et al., 1996), were purchased from Jackson Laboratory (Bar Harbor, ME). B6.129-Ahrtm1Bra/J mice were crossed with C57BL6/J mice and maintained for more than 10 generations in our facility. Heterozygous animals from different litters were crossed and homozygotes (*Ahr*+/+ and *Ahr*−/−) were used for the experiments. All animal research protocols were approved by the University of Memphis Institutional Animal Care and Use Committee and followed all guidelines and regulations. All the animals were treated humanely. Due consideration was given to alleviate any distress and discomfort.

Lipid Extraction and HPTLC

NHEKs were grown to 100% confluence and incubated in complete medium for 48 h before pretreatment with basal media for 24 h, followed by chemical treatment as indicated in basal medium supplemented with linoleic acid (10 μM) and calcium (1.2 mM) for 72 h. Lipids were extracted and measured as previously described (Kennedy et al., 2013, Tran et al., 2012). The HPTLC development system separates lipids based on polarity, the most polar lipids migrating closer to the bottom of the plate (Ponec and Weerheim, 1990). Lipid standards, including cholesterol and free fatty acid (MilliporeSigma), Cer NS (Cayman Chemical, Ann Arbor, MI), Cer AP (Evonik Industries, Essen, Germany) and GlcCers (Avanti, Birmingham, AL), were used to demonstrate separation of lipid class by polarity. The reason for migration and doublet of Cer AP standard is unknown, but may be due to differences in chain length of both sphingoid base and fatty acid moieties of this Cer class produced in *Aspergillus sp*. For this development protocol, the assignment of lipid bands was based on references (Breiden et al., 2007, Ponec et al., 2003). Lipids were quantified by densitometry (Kennedy et al., 2013, Tran et al., 2012). (Supplementary Materials and Methods)

Complex Lipid Detection

NHEKs were treated with vehicle, TCDD or tapinarof for 72 h in basal KSFM supplemented with linoleic acid (10 μM). Sample preparation and extraction were processed by Metabolon

(Morrisville, NC). Briefly, samples were subjected to a modified Bligh-Dyer extraction using methanol/water/dichloromethane in the presence of internal standards. The extracts were concentrated under nitrogen and reconstituted in 0.25 mL of 10 mM ammonium acetate dichloromethane:methanol (50:50). The extracts were transferred to inserts and placed in vials for infusion-MS analysis, performed on a Shimazdu LC with nano PEEK tubing and the Sciex SelexIon-5500 QTRAP. The samples were analyzed SelexION DMS (differential mobility spectrometry) technology (Lippa et al., 2022, Marchand et al., 2021, Ubhi, 2016, Ubhi et al., 2017). (Supplementary Materials and Methods).

ChIP-Seq Library Preparation

ChIP-seq libraries were prepared as previously described (Sutter et al., 2019). (Supplementary Materials and Methods)

ChIP-Seq Computational Analyses

Computational analyses were performed using FASTQC (http://www.bioinformatics.babraham.ac.uk/projects/fastqc/), STAR (v2.5.1) (Dobin et al., 2013) and Homer (Heinz et al., 2010). (Supplementary Materials and Methods)

Cloning, Mutagenesis, and Luciferase Assay

Constructs were prepared and luciferase assays were carried out as previously described (Sutter et al., 2011). (Supplementary Materials and Methods)

Motif Analysis

The region of AHR binding determined by ChIP-seq (Figure 2d) was scanned for putative AHR:ARNT binding sites using the motif finding software, JASPAR (Castro-Mondragon et al., 2022).

Immunoblotting, Enhanced Chemiluminescence, and Densitometry

These procedures were performed as previously described using whole cell lysis buffer (Sutter et al., 2019). (Supplementary Materials and Methods)

Statistical Analysis

Statistical analysis was performed using GraphPad Prism software, version 7.03 (GraphPad, La Jolla, CA). The statistical tests used for each analysis are described in the figure legends.

Supplementary Material

Refer to Web version on PubMed Central for supplementary material.

ACKNOWLEDGEMENTS

We thank the laboratory members, Lawrence H. Kennedy and Dylan Hammrich for their technical assistance and Zibiao Guo of the University of Memphis Feinstone Center for Genomic Research for his assistance in performing Chip-Seq analysis.

FUNDING

This work was funded by the National Institutes of Health (R01ES017014, R56ES030218, R01AR079856). The Penn Skin Biology and Diseases Resource-based Center is funded by National Institutes of Health (P30AR069589).

DATA AVAILABILITY

The ChIP-seq data are openly available in NCBI Sequence Read Archive (SRA) using the accession numbers SRR17143837 and SRR17143838.

Abbreviations:

AHR	aryl hydrocarbon receptor
TCDD	2,3,7,8-tetrachlorodibenzo-*p*-dioxin
ARNT	aryl hydrocarbon receptor nuclear transporter
EPB	epidermal permeability barrier
SC	stratum corneum
SG	stratum granulosum
ER	endoplasmic reticulum
GSL	glycosphingolipid
SM	sphingomyelin
Cer	ceramide
GlcCer or GC	glucosylceramide
LacCer	lactosylceramide
HexCer	hexosylceramide
UGCG	UDP-glucose ceramide glucotransferase
B4GALT5	beta-1,4-galactosyltransferase 5
ABCA12	ATP binding cassette subfamily A member 12
GBA1	glucosylceramidase beta
CERT1	ceramide transporter 1
SGMS	sphingomyelin synthase
SMPD1	sphingomyelin phosphodiesterase 1
SPTLC	serine palmitoyltransferase long chain
DEGS2	delta 4-desaturase, sphingolipid 2
CERS3	ceramide synthase 3

SPTSSA	serine palmitoyltransferase small subunit a
NHEKs	normal human epidermal keratinocytes
ChIP-seq	chromatin immunoprecipitation-sequencing
HPTLC	high-performance thin layer chromatography
TSS	transcriptional start site
AD	atopic dermatitis

REFERENCES

Aerts JM, Ottenhoff R, Powlson AS, Grefhorst A, van Eijk M, Dubbelhuis PF, et al. Pharmacological inhibition of glucosylceramide synthase enhances insulin sensitivity. Diabetes 2007;56(5):1341–9. [PubMed: 17287460]

Alessandrini F, Pfister S, Kremmer E, Gerber JK, Ring J, Behrendt H. Alterations of glucosylceramide-beta-glucosidase levels in the skin of patients with psoriasis vulgaris. J Invest Dermatol 2004;123(6):1030–6. [PubMed: 15610510]

Amen N, Mathow D, Rabionet M, Sandhoff R, Langbein L, Gretz N, et al. Differentiation of epidermal keratinocytes is dependent on glucosylceramide:ceramide processing. Hum Mol Genet 2013;22(20):4164–79. [PubMed: 23748427]

Bernal-Vega S, Garcia-Juarez M, Camacho-Morales A. Contribution of ceramides metabolism in psychiatric disorders. J Neurochem 2023.

Bhuju J, Olesen KM, Muenyi CS, Patel TS, Read RW, Thompson L, et al. Cutaneous Effects of In Utero and Lactational Exposure of C57BL/6J Mice to 2,3,7,8-Tetrachlorodibenzo-p-dioxin. Toxics 2021;9(8).

Boer DEC, van Smeden J, Al-Khakany H, Melnik E, van Dijk R, Absalah S, et al. Skin of atopic dermatitis patients shows disturbed beta-glucocerebrosidase and acid sphingomyelinase activity that relates to changes in stratum corneum lipid composition. Biochim Biophys Acta Mol Cell Biol Lipids 2020a;1865(6):158673. [PubMed: 32092464]

Boer DEC, van Smeden J, Bouwstra JA, Aerts J. Glucocerebrosidase: Functions in and Beyond the Lysosome. J Clin Med 2020b;9(3).

Breiden B, Gallala H, Doering T, Sandhoff K. Optimization of submerged keratinocyte cultures for the synthesis of barrier ceramides. Eur J Cell Biol 2007;86(11–12):657–73. [PubMed: 17714827]

Castro-Mondragon JA, Riudavets-Puig R, Rauluseviciute I, Lemma RB, Turchi L, Blanc-Mathieu R, et al. JASPAR 2022: the 9th release of the open-access database of transcription factor binding profiles. Nucleic Acids Res 2022;50(D1):D165–D73. [PubMed: 34850907]

Chujor CS, Feingold KR, Elias PM, Holleran WM. Glucosylceramide synthase activity in murine epidermis: quantitation, localization, regulation, and requirement for barrier homeostasis. J Lipid Res 1998;39(2):277–85. [PubMed: 9507988]

Danso M, Boiten W, van Drongelen V, Gmelig Meijling K, Gooris G, El Ghalbzouri A, et al. Altered expression of epidermal lipid bio-synthesis enzymes in atopic dermatitis skin is accompanied by changes in stratum corneum lipid composition. J Dermatol Sci 2017;88(1):57–66. [PubMed: 28571749]

Di Meglio P, Duarte JH, Ahlfors H, Owens ND, Li Y, Villanova F, et al. Activation of the aryl hydrocarbon receptor dampens the severity of inflammatory skin conditions. Immunity 2014;40(6):989–1001. [PubMed: 24909886]

Diaz-Perales A, Escribese MM, Garrido-Arandia M, Obeso D, Izquierdo-Alvarez E, Tome-Amat J, et al. The Role of Sphingolipids in Allergic Disorders. Front Allergy 2021;2:675557. [PubMed: 35386967]

Dobin A, Davis CA, Schlesinger F, Drenkow J, Zaleski C, Jha S, et al. STAR: ultrafast universal RNA-seq aligner. Bioinformatics 2013;29(1):15–21. [PubMed: 23104886]

Fling RR, Doskey CM, Fader KA, Nault R, Zacharewski TR. 2,3,7,8-Tetrachlorodibenzo-p-dioxin (TCDD) dysregulates hepatic one carbon metabolism during the progression of steatosis to steatohepatitis with fibrosis in mice. Sci Rep 2020;10(1):14831. [PubMed: 32908189]

Fujii M The Pathogenic and Therapeutic Implications of Ceramide Abnormalities in Atopic Dermatitis. Cells 2021;10(9).

Green CD, Maceyka M, Cowart LA, Spiegel S. Sphingolipids in metabolic disease: The good, the bad, and the unknown. Cell Metab 2021;33(7):1293–306. [PubMed: 34233172]

Gulbins E, Li PL. Physiological and pathophysiological aspects of ceramide. Am J Physiol Regul Integr Comp Physiol 2006;290(1):R11–26. [PubMed: 16352856]

Haas K, Weighardt H, Deenen R, Kohrer K, Clausen B, Zahner S, et al. Aryl Hydrocarbon Receptor in Keratinocytes Is Essential for Murine Skin Barrier Integrity. J Invest Dermatol 2016;136(11):2260–9. [PubMed: 27430407]

Hamanaka S, Hara M, Nishio H, Otsuka F, Suzuki A, Uchida Y. Human epidermal glucosylceramides are major precursors of stratum corneum ceramides. J Invest Dermatol 2002;119(2):416–23. [PubMed: 12190865]

Heinz S, Benner C, Spann N, Bertolino E, Lin YC, Laslo P, et al. Simple combinations of lineage-determining transcription factors prime cis-regulatory elements required for macrophage and B cell identities. Mol Cell 2010;38(4):576–89. [PubMed: 20513432]

Hu T, Todberg T, Ewald DA, Hoof I, Correa da Rosa J, Skov L, et al. Assessment of Spatial and Temporal Variation in the Skin Transcriptome of Atopic Dermatitis by Use of 1.5 mm Minipunch Biopsies. J Invest Dermatol 2022.

Janneh AH, Ogretmen B. Targeting Sphingolipid Metabolism as a Therapeutic Strategy in Cancer Treatment. Cancers (Basel) 2022;14(9).

Jennemann R, Sandhoff R, Langbein L, Kaden S, Rothermel U, Gallala H, et al. Integrity and barrier function of the epidermis critically depend on glucosylceramide synthesis. J Biol Chem 2007;282(5):3083–94. [PubMed: 17145749]

Jensen JM, Folster-Holst R, Baranowsky A, Schunck M, Winoto-Morbach S, Neumann C, et al. Impaired sphingomyelinase activity and epidermal differentiation in atopic dermatitis. J Invest Dermatol 2004;122(6):1423–31. [PubMed: 15175033]

Jin K, Higaki Y, Takagi Y, Higuchi K, Yada Y, Kawashima M, et al. Analysis of beta-glucocerebrosidase and ceramidase activities in atopic and aged dry skin. Acta Derm Venereol 1994;74(5):337–40. [PubMed: 7817665]

Kelsell DP, Norgett EE, Unsworth H, Teh MT, Cullup T, Mein CA, et al. Mutations in ABCA12 underlie the severe congenital skin disease harlequin ichthyosis. Am J Hum Genet 2005;76(5):794–803. [PubMed: 15756637]

Kennedy LH, Sutter CH, Leon Carrion S, Tran QT, Bodreddigari S, Kensicki E, et al. 2,3,7,8-Tetrachlorodibenzo-p-dioxin-mediated production of reactive oxygen species is an essential step in the mechanism of action to accelerate human keratinocyte differentiation. Toxicol Sci 2013;132(1):235–49. [PubMed: 23152189]

Kusuda S, Cui CY, Takahashi M, Tezuka T. Localization of sphingomyelinase in lesional skin of atopic dermatitis patients. J Invest Dermatol 1998;111(5):733–8. [PubMed: 9804330]

Lebwohl MG, Stein Gold L, Strober B, Papp KA, Armstrong AW, Bagel J, et al. Phase 3 Trials of Tapinarof Cream for Plaque Psoriasis. N Engl J Med 2021;385(24):2219–29. [PubMed: 34879448]

Li S, Kim HE. Implications of Sphingolipids on Aging and Age-Related Diseases. Front Aging 2021;2:797320. [PubMed: 35822041]

Lippa KA, Aristizabal-Henao JJ, Beger RD, Bowden JA, Broeckling C, Beecher C, et al. Reference materials for MS-based untargeted metabolomics and lipidomics: a review by the metabolomics quality assurance and quality control consortium (mQACC). Metabolomics 2022;18(4):24. [PubMed: 35397018]

Liu Q, Zhang L, Allman EL, Hubbard TD, Murray IA, Hao F, et al. The aryl hydrocarbon receptor activates ceramide biosynthesis in mice contributing to hepatic lipogenesis. Toxicology 2021;458:152831. [PubMed: 34097992]

Majumder S, Kono M, Lee YT, Byrnes C, Li C, Tuymetova G, et al. A genome-wide CRISPR/Cas9 screen reveals that the aryl hydrocarbon receptor stimulates sphingolipid levels. J Biol Chem 2020;295(13):4341–9. [PubMed: 32029474]

Marchand J, Guitton Y, Martineau E, Royer AL, Balgoma D, Le Bizec B, et al. Extending the Lipidome Coverage by Combining Different Mass Spectrometric Platforms: An Innovative Strategy to Answer Chemical Food Safety Issues. Foods 2021;10(6).

Menter MA, Armstrong AW, Gordon KB, Wu JJ. Common and Not-So-Common Comorbidities of Psoriasis. Semin Cutan Med Surg 2018;37(2S):S48–S51. [PubMed: 29614138]

Monies D, Anabrees J, Ibrahim N, Elbardisy H, Abouelhoda M, Meyer BF, et al. Identification of a novel lethal form of autosomal recessive ichthyosis caused by UDP-glucose ceramide glucosyltransferase deficiency. Clin Genet 2018;93(6):1252–3. [PubMed: 29417556]

Muenyi CS, Carrion SL, Jones LA, Kennedy LH, Slominski AT, Sutter CH, et al. Effects of in utero exposure of C57BL/6J mice to 2,3,7,8-tetrachlorodibenzo-p-dioxin on epidermal permeability barrier development and function. Environ Health Perspect 2014;122(10):1052–8. [PubMed: 24904982]

Nault R, Fader KA, Kopec AK, Harkema JR, Zacharewski TR, Luyendyk JP. From the Cover: Coagulation-Driven Hepatic Fibrosis Requires Protease Activated Receptor-1 (PAR-1) in a Mouse Model of TCDD-Elicited Steatohepatitis. Toxicol Sci 2016;154(2):381–91. [PubMed: 27613713]

Nomoto K, Itaya Y, Watanabe K, Yamashita T, Okazaki T, Tokudome Y. Epidermal permeability barrier function and sphingolipid content in the skin of sphingomyelin synthase 2 deficient mice. Exp Dermatol 2018;27(8):827–32. [PubMed: 29345004]

Norlen L, Lundborg M, Wennberg C, Narangifard A, Daneholt B. The Skin's Barrier: A Cryo-EM Based Overview of its Architecture and Stepwise Formation. J Invest Dermatol 2022;142(2):285–92. [PubMed: 34474746]

Paller AS, Stein Gold L, Soung J, Tallman AM, Rubenstein DS, Gooderham M. Efficacy and patient-reported outcomes from a phase 2b, randomized clinical trial of tapinarof cream for the treatment of adolescents and adults with atopic dermatitis. J Am Acad Dermatol 2021;84(3):632–8. [PubMed: 32502588]

Ponec M, Weerheim A. Retinoids and lipid changes in keratinocytes. Methods Enzymol 1990;190:30–41. [PubMed: 2087181]

Ponec M, Weerheim A, Lankhorst P, Wertz P. New acylceramide in native and reconstructed epidermis. J Invest Dermatol 2003;120(4):581–8. [PubMed: 12648220]

Rabionet M, Gorgas K, Sandhoff R. Ceramide synthesis in the epidermis. Biochim Biophys Acta 2014;1841(3):422–34. [PubMed: 23988654]

Reza S, Ugorski M, Suchański J. Glucosylceramide and galactosylceramide, small glycosphingolipids with significant impact on health and disease. Glycobiology 2021;31(11):1416–34. [PubMed: 34080016]

Saurat JH, Kaya G, Saxer-Sekulic N, Pardo B, Becker M, Fontao L, et al. The cutaneous lesions of dioxin exposure: lessons from the poisoning of Victor Yushchenko. Toxicol Sci 2012;125(1):310–7. [PubMed: 21998131]

Schmidt JV, Su GH, Reddy JK, Simon MC, Bradfield CA. Characterization of a murine Ahr null allele: involvement of the Ah receptor in hepatic growth and development. Proc Natl Acad Sci U S A 1996;93(13):6731–6. [PubMed: 8692887]

Schmuth M, Man MQ, Weber F, Gao W, Feingold KR, Fritsch P, et al. Permeability barrier disorder in Niemann-Pick disease: sphingomyelin-ceramide processing required for normal barrier homeostasis. J Invest Dermatol 2000;115(3):459–66. [PubMed: 10951284]

Schwingen J, Kaplan M, Kurschus FC. Review-Current Concepts in Inflammatory Skin Diseases Evolved by Transcriptome Analysis: In-Depth Analysis of Atopic Dermatitis and Psoriasis. Int J Mol Sci 2020;21(3).

Sidransky E, Sherer DM, Ginns EI. Gaucher disease in the neonate: a distinct Gaucher phenotype is analogous to a mouse model created by targeted disruption of the glucocerebrosidase gene. Pediatr Res 1992;32(4):494–8. [PubMed: 1437405]

Smith SH, Jayawickreme C, Rickard DJ, Nicodeme E, Bui T, Simmons C, et al. Tapinarof Is a Natural AhR Agonist that Resolves Skin Inflammation in Mice and Humans. J Invest Dermatol 2017;137(10):2110–9. [PubMed: 28595996]

Sutter CH, Bodreddigari S, Campion C, Wible RS, Sutter TR. 2,3,7,8-Tetrachlorodibenzo-p-dioxin increases the expression of genes in the human epidermal differentiation complex and accelerates epidermal barrier formation. Toxicol Sci 2011;124(1):128–37. [PubMed: 21835898]

Sutter CH, Olesen KM, Bhuju J, Guo Z, Sutter TR. AHR Regulates Metabolic Reprogramming to Promote SIRT1-Dependent Keratinocyte Differentiation. J Invest Dermatol 2019;139(4):818–26. [PubMed: 30393078]

Sutter CH, Yin H, Li Y, Mammen JS, Bodreddigari S, Stevens G, et al. EGF receptor signaling blocks aryl hydrocarbon receptor-mediated transcription and cell differentiation in human epidermal keratinocytes. Proc Natl Acad Sci U S A 2009;106(11):4266–71. [PubMed: 19255421]

Thyssen JP, Halling A-S, Schmid-Grendelmeier P, Guttman-Yassky E, Silverberg JI. Comorbidities of atopic dermatitis—what does the evidence say? Journal of Allergy and Clinical Immunology 2023.

Toncic RJ, Jakasa I, Hadzavdic SL, Goorden SM, Vlugt KJG, Stet FS, et al. Altered Levels of Sphingosine, Sphinganine and Their Ceramides in Atopic Dermatitis Are Related to Skin Barrier Function, Disease Severity and Local Cytokine Milieu. Int J Mol Sci 2020;21(6).

Tran QT, Kennedy LH, Leon Carrion S, Bodreddigari S, Goodwin SB, Sutter CH, et al. EGFR regulation of epidermal barrier function. Physiol Genomics 2012;44(8):455–69. [PubMed: 22395315]

Tsoi LC, Rodriguez E, Degenhardt F, Baurecht H, Wehkamp U, Volks N, et al. Atopic Dermatitis Is an IL-13-Dominant Disease with Greater Molecular Heterogeneity Compared to Psoriasis. J Invest Dermatol 2019;139(7):1480–9. [PubMed: 30641038]

Tsuji G, Hashimoto-Hachiya A, Kiyomatsu-Oda M, Takemura M, Ohno F, Ito T, et al. Aryl hydrocarbon receptor activation restores filaggrin expression via OVOL1 in atopic dermatitis. Cell Death Dis 2017;8(7):e2931. [PubMed: 28703805]

Uberoi A, Bartow-McKenney C, Zheng Q, Flowers L, Campbell A, Knight SAB, et al. Commensal microbiota regulates skin barrier function and repair via signaling through the aryl hydrocarbon receptor. Cell Host Microbe 2021;29(8):1235–48 e8. [PubMed: 34214492]

Ubhi BK. Novel chemical standards kits enable facile lipid quantitation. SCIEX Technical Application Note 2016; RUO-MKT-02–3879-A.

Ubhi BK, Conner A, Duchoslav E, Evans A, Robinson R, Baker PRS, et al. A novel lipid screening platform that provides a complete solution for lipidomics research. SCIEX Technical Application Note 2017; RUO-MKT-02–2871-A.

Uchida Y, Park K. Ceramides in Skin Health and Disease: An Update. Am J Clin Dermatol 2021;22(6):853–66. [PubMed: 34283373]

van den Bogaard EH, Bergboer JG, Vonk-Bergers M, van Vlijmen-Willems IM, Hato SV, van der Valk PG, et al. Coal tar induces AHR-dependent skin barrier repair in atopic dermatitis. J Clin Invest 2013;123(2):917–27. [PubMed: 23348739]

van Smeden J, Janssens M, Gooris GS, Bouwstra JA. The important role of stratum corneum lipids for the cutaneous barrier function. Biochim Biophys Acta 2014;1841(3):295–313. [PubMed: 24252189]

Yamaji T, Hanada K. Sphingolipid metabolism and interorganellar transport: localization of sphingolipid enzymes and lipid transfer proteins. Traffic 2015;16(2):101–22. [PubMed: 25382749]

Yamashita T, Wada R, Sasaki T, Deng C, Bierfreund U, Sandhoff K, et al. A vital role for glycosphingolipid synthesis during development and differentiation. Proc Natl Acad Sci U S A 1999;96(16):9142–7. [PubMed: 10430909]

Yokose U, Ishikawa J, Morokuma Y, Naoe A, Inoue Y, Yasuda Y, et al. The ceramide [NP]/[NS] ratio in the stratum corneum is a potential marker for skin properties and epidermal differentiation. BMC Dermatol 2020;20(1):6. [PubMed: 32867747]

Zhao H, Przybylska M, Wu IH, Zhang J, Maniatis P, Pacheco J, et al. Inhibiting glycosphingolipid synthesis ameliorates hepatic steatosis in obese mice. Hepatology 2009;50(1):85–93. [PubMed: 19444873]

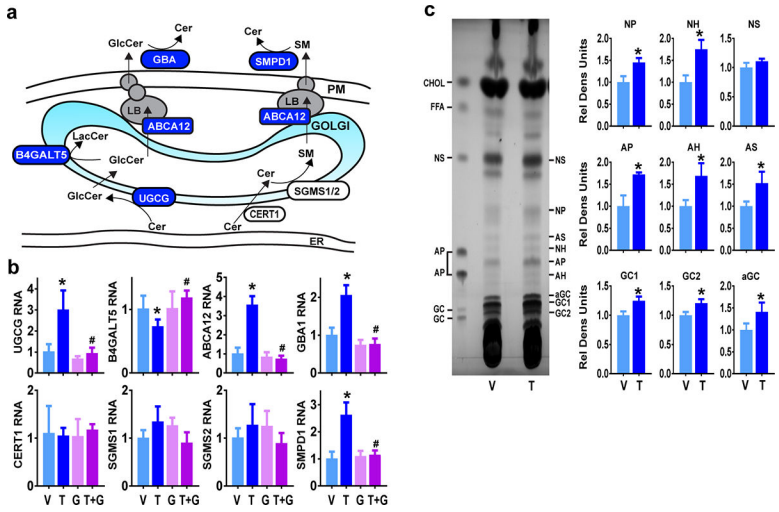

Figure 1. The effects of AHR activation on the expression of ceramide (Cer) metabolic and transport genes in epidermal keratinocytes.

(**a**) Simplified diagram of epidermal Cer metabolism. Certain Cers formed in the endoplasmic reticulum (ER) (*de novo* synthesis) are transported directly into the *trans* Golgi lumen via ceramide transporter (CERT1) and converted to sphingomyelin (SM) by SGMS1/2. Others are glucosylated by UGCG at the surface of the *cis/medial* Golgi to form GlcCer. [See references (Fujii, 2021, Yamaji and Hanada, 2015) for detailed discussion of ceramide synthesis and trafficking.] In the Golgi of the epidermis, a small amount of GlcCer is converted to LacCer by B4GALT5. Most GlcCers and SMs are trafficked via the lamellar body network [(LB) depicted in grey] through the plasma membrane (PM) into the extracellular space of the secretory cells of the stratum granulosum. Here the acid enzymes, GBA1 and SMPD1, remove glucose or phosphocholine, respectively, to regenerate the numerous hydrophobic ceramides that make up the lipid lamellae of the stratum corneum. While the phosphodiesterase activity of SMPD1 synthesizes only the NS and AS subclasses of Cers, GBA1 hydrolyses most GlcCers and acylGlcCers to generate the other Cers (Fujii, 2021). The expression of enzymes and transporters colored in blue are affected by activation of the AHR. (**b**) Assessment of AHR-mediated effects on RNA expression of Cer metabolism and transport genes. NHEKs were treated (24 h) with either vehicle (V, 0.2% DMSO), TCDD (T, 10 nM, agonist), GNF351 (G, 100 nM, antagonist) or the combination of TCDD and GNF351 (T+G). Real-time qPCR was used to determine the relative RNA expression of UGCG, B4GALT5, ABCA12, GBA1, CERT1, SGMS1, SGMS2 and SMPD1. Levels of RNA [mean (n=4), +/− standard deviation (SD)] are expressed relative to the vehicle, given a value of one. The * indicates a significant difference from the vehicle sample and the # indicates a significant difference from the TCDD-alone sample using a two-way ANOVA followed by Tukey's multiple comparisons test, $p<0.05$. (**c**) Levels of glucosylated (GC1, GC2 and aGC) and non-glucosylated Cers (NP, NH, NS, AP, AH, and AS) in keratinocytes treated with TCDD. NHEKs were treated (72 h) with vehicle (V, 0.1% DMSO) or TCDD (T, 10 nM). Left, representative HPTLC separation of lipid classes using a ceramide development system. Lipid standards (far-left lane) were used to demonstrate separation of lipid classes by polarity. Identity of ceramides is based on their order as described (Breiden et al., 2007, Ponec et al., 2003). (See Supplemental Table S1 for naming

of the ceramides.) Right, quantitation by densitometry of the indicated lipid bands [mean (n=3), +/− standard deviation (SD)] are expressed relative to the vehicle, given a value of one. The * indicates a significant difference from the vehicle sample using a two-tailed unpaired t-test, $p<0.05$.

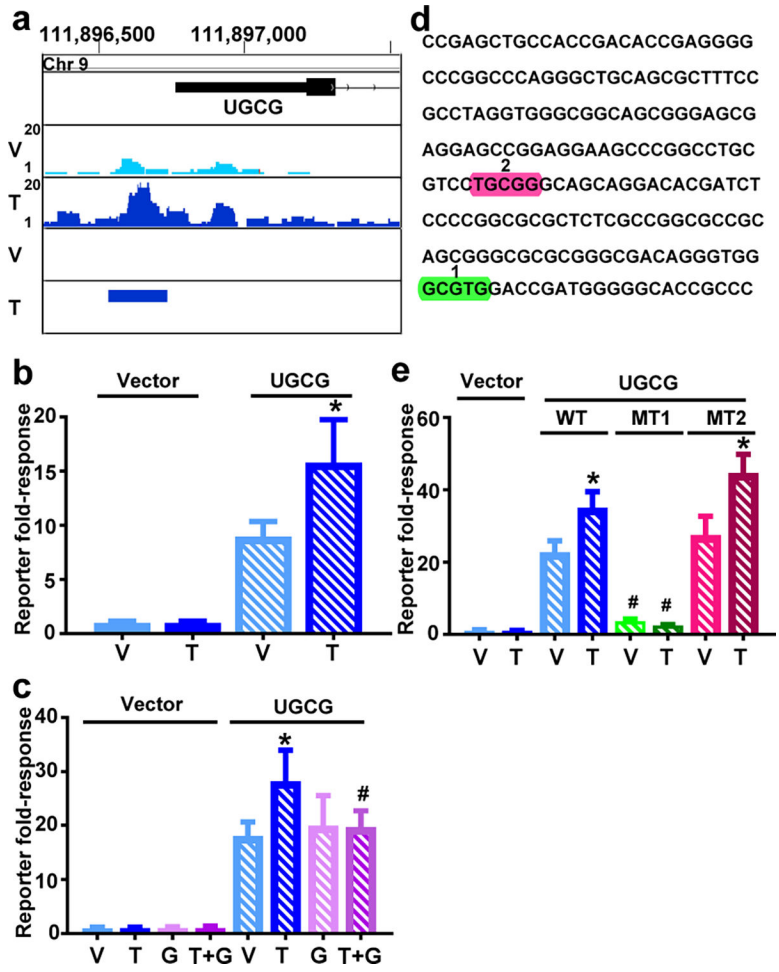

Figure 2. Transcriptional regulation of UGCG by activation of the AHR with TCDD.

(**a**) Chromatin immunoprecipitation sequencing analyses identified a region near the TSS of UGCG as a target of AHR binding. The top set of tracks of this panel displays the chromosomal location of the mapped reads. Below are tracks displaying the peak height in the vehicle (V, 0.1% DMSO, light blue)- and TCDD-treated (T, 10 nM, bright blue) samples with the scale of the read depth indicated to the left. The next set of tracks displays the statistical analyses, where statistically significant peaks are identified with a rectangle (FDR=0.001). (**b**) NHEKs transfected with the indicated luciferase reporters, empty vector (Vector) or the UGCG region identified in (a) (UGCG), were treated (24 h) with either the vehicle (V, 0.1% DMSO) or TCDD (T, 10 nM). Reporter fold-responses [mean (n=6), +/− standard deviation (SD)] were graphed. The * indicates a significant difference from the vehicle sample using a two-tailed unpaired t-test, $p<0.05$. (**c**) NHEKs transfected with the indicated luciferase reporters, empty vector or the UGCG region identified in (a), were treated (24 h) with either the vehicle (V, 0.2% DMSO), TCDD (T, 10 nM), GNF351 (G, 100 nM) or the combination of TCDD and GNF351 (T+G). Reporter fold-responses [mean (n=6), +/− standard deviation (SD)] were graphed. The * indicates a significant difference from the vehicle samples and the # indicates a significant difference from the TCDD-alone samples using a two-way ANOVA followed by Tukey's multiple comparisons

test, $p<0.05$. (**d**) DNA sequence corresponding to region of AHR binding depicted in (a). The locations of the two sites of site-directed mutagenesis are indicated by highlighting and the numbers 1 and 2. (**e**) NHEKs transfected with the indicated luciferase reporters, empty vector, the UGCG region identified in (d, wild type, WT), or UGCG mutant (MT) 1 or 2 were treated (24 h) with either the vehicle (V, 0.1% DMSO) or TCDD (T, 10 nM). Reporter fold-responses [mean (n=6), +/− standard deviation (SD)] were graphed. The * indicates a significant difference from the vehicle samples within the same specific construct and the # indicates a significant difference from the WT construct within the same treatment using a two-way ANOVA followed by Tukey's multiple comparisons test, $p<0.05$.

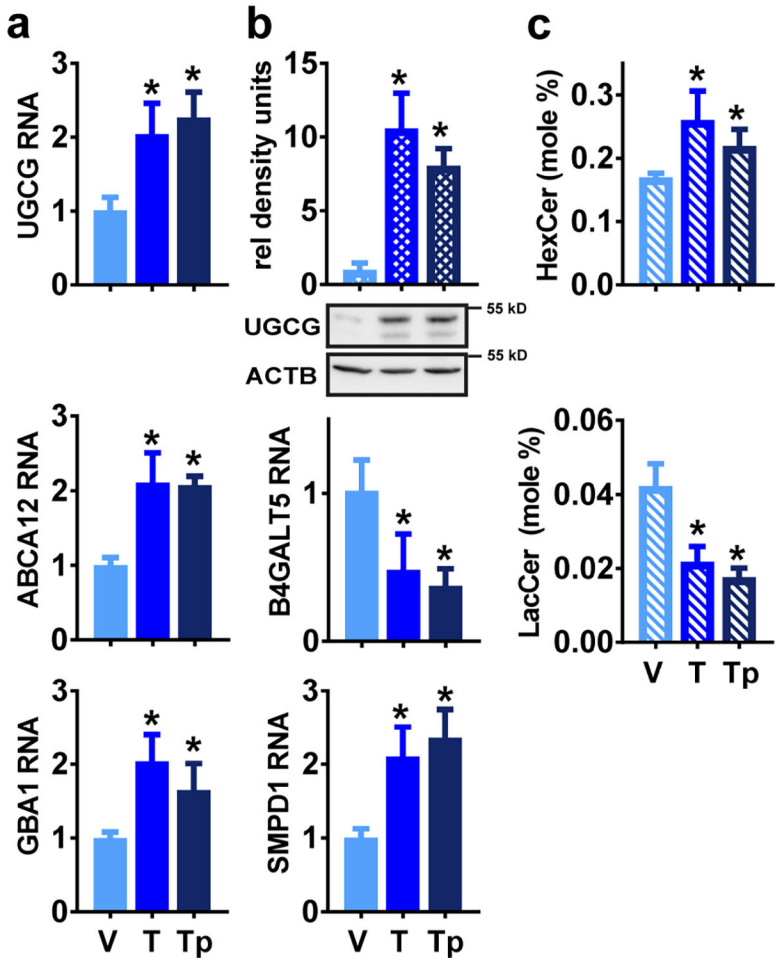

Figure 3. Effects of TCDD- or tapinarof-activated AHR on UGCG, its associated metabolic pathways and Cer levels.

(**a**) NHEKs were treated (24 h) with either vehicle (V, 0.1% DMSO, light blue solid bar), TCDD (T, 10 nM, bright blue solid bar), or tapinarof (Tp, 3 μM, dark blue solid bar). Real-time qPCR was used to determine the relative RNA expression of UGCG, ABCA12, GBA1, B4GALT5 and SMPD1. Levels of RNA [mean (n=4), +/− standard deviation (SD)] are expressed relative to the vehicle, given a value of one. (**b**) NHEKs were treated (48 h) with either the vehicle (V, 0.1% DMSO, light blue stippled bar), TCDD (T, 10 nM, bright blue stippled bar), or tapinarof (Tp, 3 μM, dark blue stippled bar). Levels of UGCG protein detected by immunoblot [mean (n=3), +/− standard deviation (SD)] were quantitated by densitometry and normalized with levels of ACTB before being expressed relative to the vehicle, given a value of one. (**c**) NHEKs were treated (72 h) with either the vehicle (V, 0.1% DMSO, light blue diagonal bar), TCDD (T, 10 nM, bright blue diagonal bar), or tapinarof (Tp, 3 μM, dark blue diagonal bar). Levels of hexosylceramides (HexCer, sum of glucosyl- and galactosylceramides) and lactosylceramides (LacCer) [mean (n=6), +/− standard deviation (SD)] were expressed as a percentage of the total lipids in the samples. The * indicates a significant difference from the vehicle samples using a one-way ANOVA followed by Tukey's multiple comparisons test, $p<0.05$.

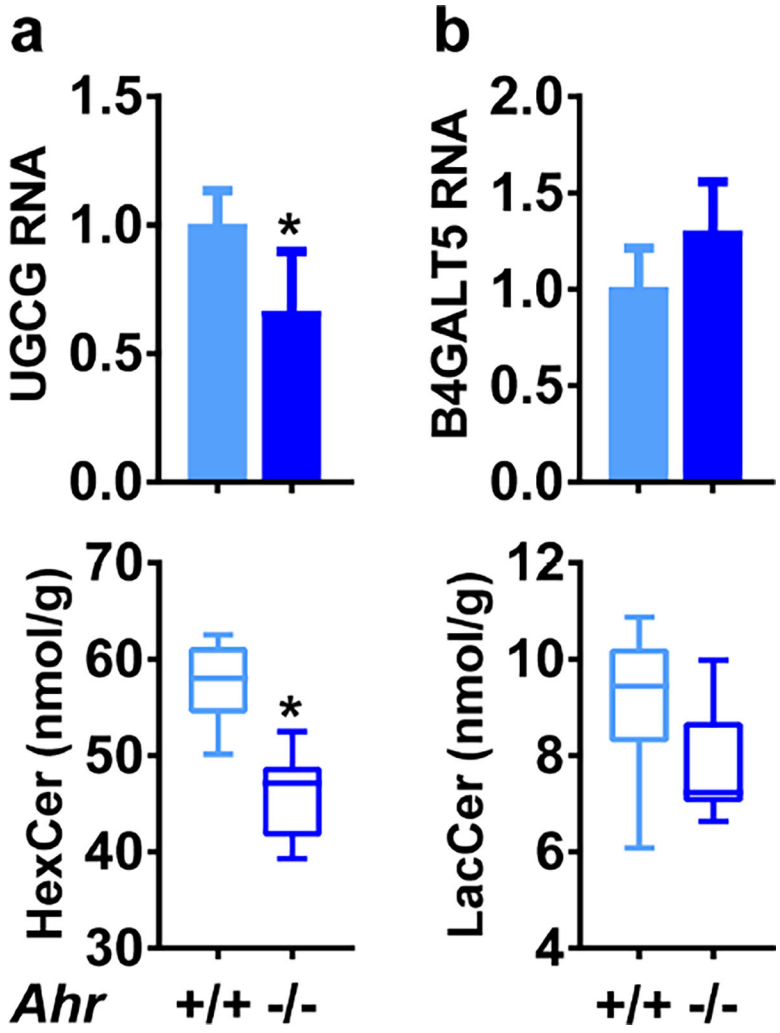

Figure 4. Expression of UGCG and B4GALT5 in *Ahr* WT and *Ahr* knock-out mice.

Real-time qPCR was used to determine the relative RNA expression of UGCG (**a, upper**) and B4GALT5 (**b, upper**) from skin of *Ahr* WT (+/+) and knock-out (−/−) mice. Levels of hexosylceramides (HexCer) **a, lower**) and lactosylceramides (LacCer, **b, lower**) [mean (n=8), +/− standard deviation (SD)] were measured in *Ahr* WT (+/+) and knock-out (−/−) mice skin samples. The * indicates a significant difference from WT samples using a two-tailed unpaired t-test, $p<0.05$.